

Electrostatic Control of Divertor Flows in a Stellarator

R. P. Doerner, D. T. Anderson, W. N. G. Hitchon, P. G. Matthews, and J. L. Shohet
Torsatron/Stellarator Laboratory, University of Wisconsin-Madison, Madison, Wisconsin 53706
 (Received 17 October 1988)

An electrostatic method for controlling diverted particle fluxes in a stellarator has been demonstrated. Potentials applied to a defined set of divertor targets (shields) in contact with diverted flux bundles results in redistribution of plasma flow to any given divertor. Examination of the edge magnetic topology shows that $\mathbf{E} \times \mathbf{B}$ drifts just outside the last-closed magnetic surface account for the alteration of the diverted particle flows.

PACS numbers: 52.55.Hc

Experimental evidence of divertor structure has been observed in many stellarators.^{1,2} Stellarator divertors usually spread the diverted flux over large regions.³ An externally applied vertical magnetic field has been used to globally alter the divertor pattern in a stellarator.⁴ We present here a method using electrostatic fields which provides local control of diverted particle fluxes in the Interchangeable Module Stellarator (IMS).

IMS is an $l=3$, seven-field-period modular stellarator with a 40 cm major radius and a 4.5 cm average plasma radius.⁵ Outside the last-closed magnetic surface (LCMS) is a region of ergodic field lines which extends radially for about 5 mm. Beyond this region, field-line trajectories quickly coalesce to form 63 diverted flux bundles. This divertor structure has been observed both computationally⁶ and experimentally.⁷ Electrically isolated stainless-steel shields placed at the locations of each of the 63 emergent bundles in IMS are used to monitor the diverted plasma flow as well as to apply an electrostatic bias to specific divertor bundles. The location of each shield is identified by both the coil support ring on which it is mounted and the poloidal angle at which it is positioned on the coil support ring as shown in Fig. 1 (e.g., S8-340).

Tracing the magnetic field lines from a given divertor shield back to a reference surface 5 mm beyond the LCMS gives an origin "map" of the field lines comprising that divertor bundle. An origin mapping of all nine divertors in one field period is presented in Fig. 2. Any point on the reference surface is connected by field lines to at most two divertors. By following field lines parallel to the direction of the magnetic field a diagram is generated which indicates the areas of the launch surface that are connected to the various divertors [Fig. 2(a)]. Figure 2(b) shows a similar map generated by following field lines in the opposite direction. Superimposing Figs. 2(a) and 2(b) reveals that the field lines connecting to a given divertor originate mainly from a continuous toroidal strip on the reference surface. It has been experimentally confirmed by launching ion-acoustic waves beyond the LCMS and monitoring the divertor shields to detect the wave⁸ that the plasma flows closely follow this mapping in IMS. The ion-acoustic wave propagation

measurements⁹ were also used to obtain a value for the diverted plasma flow velocity.

Measurements of the floating potential just outside the LCMS were taken during shield-biasing experiments. The regions outside the LCMS which connect to the biased divertor shield exhibited changes in the floating potential as the voltage on the divertor shield was varied. Changes in the floating potential of up to T_e , the electron temperature, were observed. A probe inserted in other origin regions, not connected to the biased shield, showed no appreciable change in floating potential when the same shield's bias was varied. Central plasma parameters also exhibited no changes during divertor-shield biasing. Measurements of the space potential showed changes similar to those in the floating potential.

Figure 3(b) shows the change in the diverted ion current to a gridded energy analyzer within a divertor when an adjacent divertor shield's bias voltage was varied. The change in current is strongly correlated with the floating potential change near the separatrix [Fig. 3(a)]. As the change in the floating potential grows larger, with increased dc bias, an electric field develops between the biased and unbiased regions of the launch

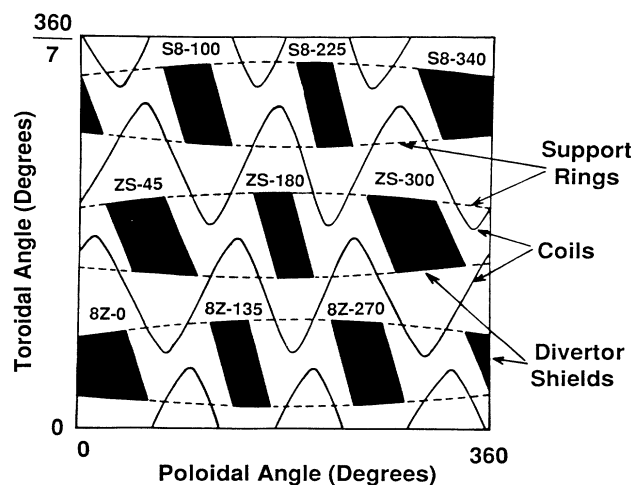


FIG. 1. Schematic diagram of one field period indicating divertor-shield nomenclature.

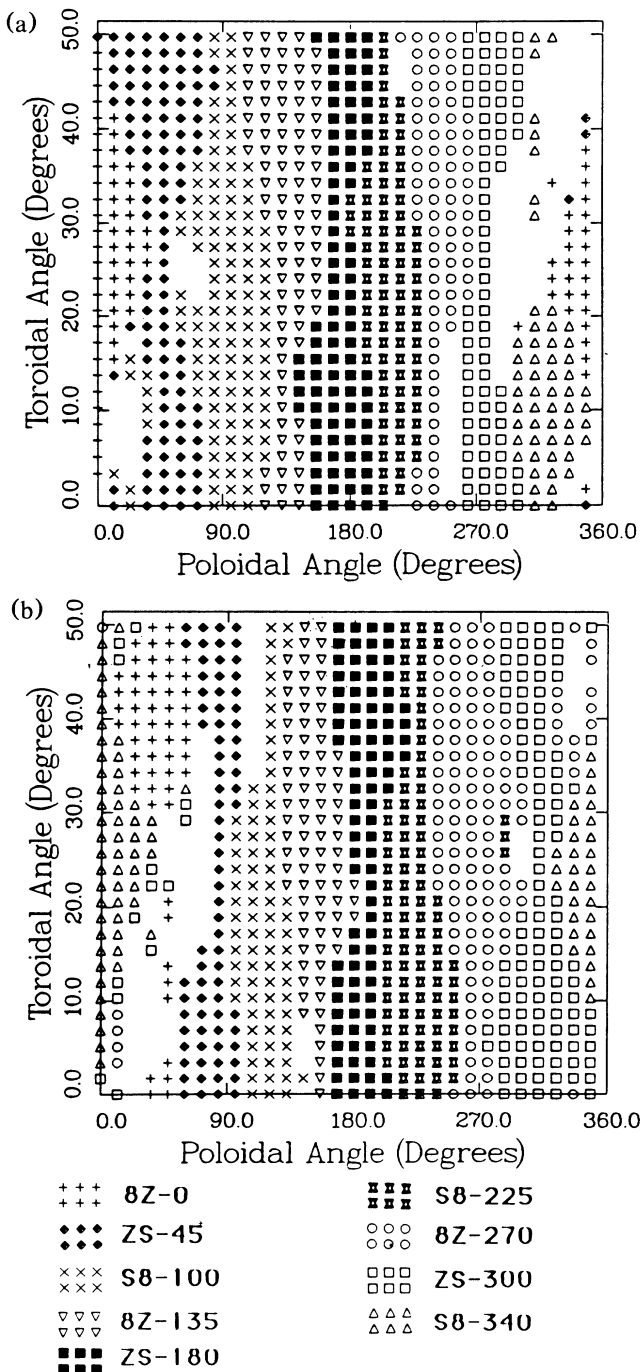


FIG. 2. Each of the nine divertor-origin locations in one field period on the launch surface: field lines (a) followed in the direction of B and (b) followed opposite to the direction of B .

surface (outside the separatrix) and the diverted particle current changes. When the change in the floating potential saturates (at T_e volts) in the biased-origin region, no further changes are observed in the diverted particle currents.

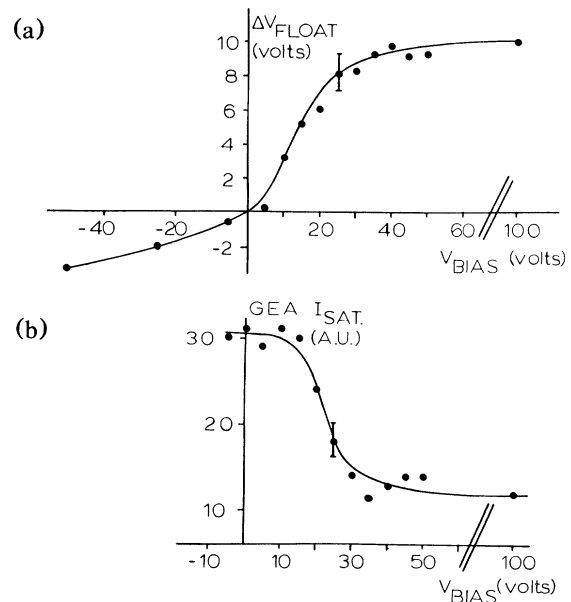


FIG. 3. (a) The change in the potential near the last-closed magnetic surface and (b) the ion-saturation current to a divertor, as functions of the bias potential.

A positive 50-V potential was applied to the divertor shield in each field period that is located at a poloidal angle of 340° (i.e., the S8-340 shield, see Fig. 1). The ion-saturation current to each divertor within one field period was measured. The ion-saturation current to the shield located at a poloidal angle of 300° (the ZS-300 shield) and the shield located at a poloidal angle of 0° (the 8Z-0 shield) exhibited changes. The ion-saturation current to the other shields showed no appreciable changes during biasing of the S8-340 shields. Referring again to Fig. 2, the ZS-300 and the 8Z-0 origins are seen to flank the biased S8-340 origin. The diverted ion current to the ZS-300 divertor rises abruptly from 10.5 to 15.7 mA when the bias is applied to the S8-340 divertor shields. At the same time, the diverted ion current to the 8Z-0 divertor abruptly decreases from 8.0 to 2.0 mA when the bias voltage is applied.

Figure 4 shows the experimental data obtained with this shield-biasing configuration. The two traces labeled ZS-300 and 8Z-0 monitor the ion-saturation current collected by each of these divertor shields. The bias is switched on halfway through the discharge. The current to each divertor clearly exhibits an abrupt change when the bias is applied to the S8-340 shields. The total current collected by the biased shield is the trace labeled I_{bias} . The line-averaged density does not change appreciably over the course of the plasma discharge. Particularly, it does not change when the bias is applied.

From these data, the diverted ion current decreases to the divertor whose origin strip is located on the positive-poloidal-angle side of the biased origin. The current increases to the divertor whose origin is located on the

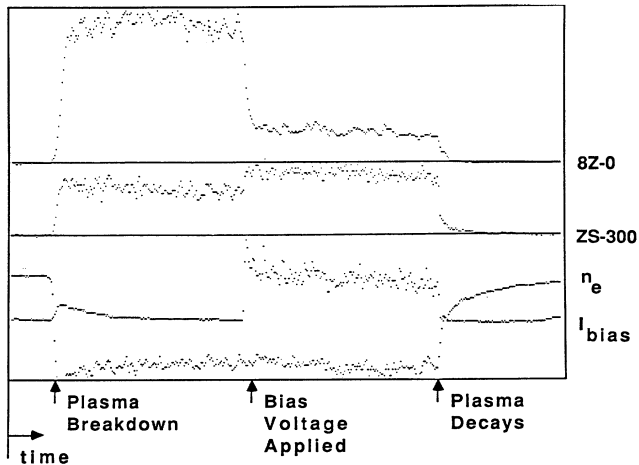


FIG. 4. Experimental data showing changes in ion-saturation current to two divertors during +50-V biasing of the S8-340 divertor shield. The density is the nearly flat trace near the bottom of the figure.

negative-poloidal-angle side of the biased origin. This trend persists even when other sets of divertor shields are biased. Since the decrease in current to one monitored divertor approximately equals the increase in current to the other monitored divertor, and since the currents to remote divertors exhibit only minimal changes, we conclude that the redistribution of flux is predominantly localized to the origin regions bordering the biased-origin region.

The perpendicular conductivity of the IMS edge plasma is several orders of magnitude too small to account for the observed changes. Reversing the direction of the coil currents leaves the structure of the magnetic field unchanged. Reversing the direction of the magnetic field should not directly change the electric field structure along a magnetic field line. Thus, one would expect to measure identical alterations to the diverted particle flows (at least to lowest order), if parallel conduction is the dominant mechanism responsible. On the other hand, reversing the direction of the magnetic field reverses the direction of any $\mathbf{E} \times \mathbf{B}$ drifts. If an $\mathbf{E} \times \mathbf{B}$ drift is responsible for the observed alterations, one would expect to see a reversal of the trend described above.

The measured potential changes (just outside the LCMS) due to shield biasing indicate the formation of an electric field having both radial and poloidal components. The radial component of the electric field acts to produce a poloidal drift (which pushes plasma poloidally around from one origin to a neighboring origin). The poloidal electric field component results in a radial $\mathbf{E} \times \mathbf{B}$ drift. The radial $\mathbf{E} \times \mathbf{B}$ drift resulting from shield biasing is the same order of magnitude as the measured plasma flow velocity through the divertors.⁸ This radial drift acts to pull plasma out from near the LCMS on one side of the biased origin (i.e., the drift is outward) and to

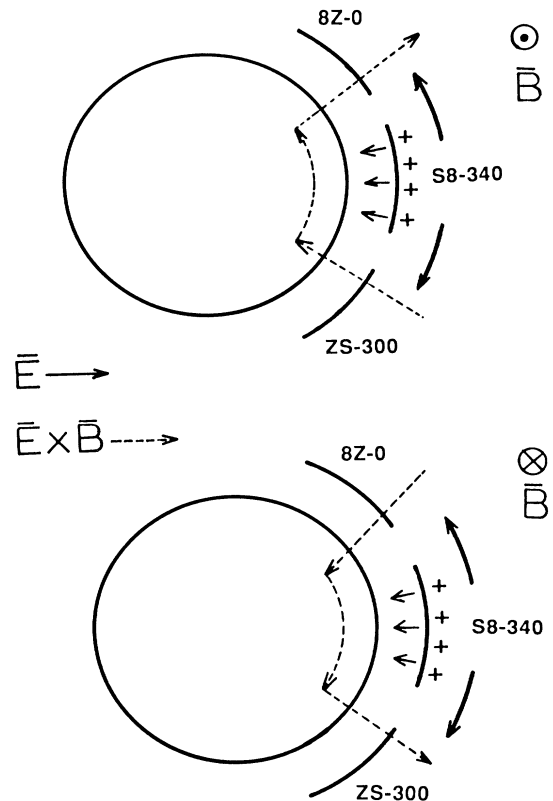


FIG. 5. Pictorial representation of electric fields and $\mathbf{E} \times \mathbf{B}$ drift directions resulting from positive biasing of the S8-340 divertor shield.

retard the flow of plasma out of the region near the LCMS on the other side (the drift is inward). The poloidal and radial electric fields thus act in concert.

Repeating the measurement with the S8-340 divertor shield biased to +50 V, but with the oppositely directed (i.e., "negative") magnetic field, does show a reversal of the change in the diverted ion current to both of the divertors described previously (the ZS-300 and the 8Z-0 divertors). This is consistent with an $\mathbf{E} \times \mathbf{B}$ drift acting on the diverted plasma. The diverted ion current to the ZS-300 divertor decreases by 5.2 mA, whereas with a "positively" directed magnetic field, the current increased by 5.2 mA. The change in the diverted ion current to the 8Z-0 divertor also reverses, increasing by 6.4 mA, whereas it had decreased (with a positively directed magnetic field) by 6.0 mA. The fields and drift directions are pictorially represented in Fig. 5.

Further confirmation of the $\mathbf{E} \times \mathbf{B}$ drift hypothesis has been obtained by operating IMS with a central magnetic field strength of 5.8 kG instead of the normal 2.6 kG. Measurements of the alterations in the diverted ion currents were made at the higher-field setting. The higher power available from the 17-GHz source (20 kW) and operation at 5.8 kG allowed the creation of plasma

TABLE I. Shield-biasing results during plasma operation at central magnetic fields of 2.6 and 5.8 kG. ΔI denotes the measured change of diverted ion current during shield biasing.

B (kG)	n_e (cm^{-3})	T_e (eV)	E (V/cm)	E/B (cm/s)	V_{flow} (cm/s)	$\frac{E/B}{V_{\text{flow}}}$	ΔI (%)
2.6	2×10^{11}	8-12	8	3.1×10^5	1.2×10^6	0.26	-62
5.8	4.6×10^{11}	20-25	21	3.6×10^5	2.0×10^6	0.18	-40

with ~ 2.5 times the density and electron temperature of the lower-field plasmas. The differences between the plasma parameters in the two cases provides an excellent means of verifying the $\mathbf{E} \times \mathbf{B}$ drift hypothesis. Table I summarizes the parameters of the two different regimes of operation and indicates the percent change in the diverted ion current to the same divertor during shield biasing for each configuration.

The higher electron temperature during 5.8-kG operation is seen to effect the shield-biasing measurements in two ways. First, the increased temperature permits a higher potential to be maintained in the origin strip. Second, the larger electron energy increases the ion-sound speed and, therefore, also increases the measured diverted plasma flow velocity. The imposed $\mathbf{E} \times \mathbf{B}$ drift velocity is quite similar for the two cases (as a result of increases in both E and B for the 5.8-kG case). However, the ratio of the $\mathbf{E} \times \mathbf{B}$ drift velocity to the diverted plasma flow velocity is observed to be less in the 5.8-kG case. The percent change in the diverted ion current during shield biasing is seen to scale closely with the ratio of the $\mathbf{E} \times \mathbf{B}$ drift velocity to the diverted plasma flow velocity.

These scaling results indicate that the dominant mechanism responsible for the redistribution of particle flux through the IMS divertors appears to be the $\mathbf{E} \times \mathbf{B}$ drift of the diverted plasma. This scaling indicates that this technique can be applicable to other larger stellarator devices. The plasma which is inhibited from flowing through the divertor (by the minor radially inward $\mathbf{E} \times \mathbf{B}$ drift) is directed to a location where the outward $\mathbf{E} \times \mathbf{B}$

drift enhances plasma flow through that divertor. This shows that it is possible to alter the diverted plasma flow patterns in a stellarator, by use of potentials applied to remote material surfaces in the edge region, without affecting the central plasma confinement properties.

This work was supported by the U. S. Department of Energy Grant No. DE-FG02-86-ER53216.A004 and Oak Ridge National Laboratory Contract No. 19X-3591-C.

¹V. S. Voitsenya, A. Y. Voloshko, E. M. Lats'ko, S. I. Solodovchenko, and A. F. Shtan', Nucl. Fusion **19**, 1241 (1979).

²O. Motojima, A. Iiyoshi, and K. Uo, Nucl. Fusion **15**, 985 (1975).

³C. Gourdon, D. Marty, E. K. Maschke, and J. Touche, Nucl. Fusion **11**, 161 (1971).

⁴R. P. Doerner, D. T. Anderson, F. S. B. Anderson, P. G. Matthews, and J. L. Shohet, Nucl. Fusion **28**, 1901 (1988).

⁵D. T. Anderson, J. A. Derr, and J. L. Shohet, IEEE Trans. Plasma Sci. **9**, 212 (1981).

⁶J. A. Derr and J. L. Shohet, IEEE Trans. Plasma Sci. **9**, 234 (1981).

⁷R. P. Doerner, D. T. Anderson, F. S. B. Anderson, J. L. Shohet, and J. N. Talmadge, Phys. Fluids **29**, 3807 (1986).

⁸R. P. Doerner, Ph.D. thesis, University of Wisconsin-Madison, 1988 (unpublished).

⁹K. Ando *et al.*, in *Proceedings of the Fifth International Conference on Plasma Physics and Controlled Nuclear Fusion Research, Tokyo, Japan, 1974* (IAEA, Vienna, 1975), Vol. 1, p. 103.